Journal of Nuclear Materials 406 (2010) 277–284

Contents lists available at ScienceDirect

Journal of Nuclear Materials

journal homepage: www.elsevier.com/locate/jnucmat

On the oxidation of (U, Pu)C fuel: Experimental and kinetic aspects, practical issues

F. Mazaudier [a,*], C. Tamani [a], A. Galerie [b], Y. Marc [a]

[a] CEA, DEN, DEC, 13108 St. Paul-lez-Durance, France
[b] SIMAP, PHELMA, Grenoble INP, BP 75, 38402 St. Martin-d'Hères, France

ARTICLE INFO

Article history:
Received 18 February 2010
Accepted 26 July 2010

ABSTRACT

The oxidation of mixed (U, Pu) carbide fuel was studied to meet some of the general requirements applicable to the back- and front-end of the nuclear fuel cycle. Data are unfortunately scarce in this field. Based on an experimental study and a kinetic treatment, it was proved that the oxidation of solid or powdered mixed carbide fuel does not involve any unwanted kinetic transition and does not have the intrinsic ability to self-sustain. We never observed the formation of a protective oxide layer on the samples. The oxidation products were always low-density, finely-divided oxide powder expanding and tending to slow down the process. The low thermal activation observed demonstrates the key role of gas transport when using powders. Practical solutions have been derived from this work.

1. Introduction

The mixed (U, Pu) carbide fuel is a promising candidate for Gen IV reactors thanks to a heavier atom density and better thermal conductivity when compared with oxide fuel. Managing the oxidation of (U, Pu)C fuel is one of the main questions underlying: (i) the safety risk analysis for the back-end which needs to reprocess scraps and spent fuel (via the Purex® process), (ii) the regulatory requirements for safe storage and, currently, and (iii) the standard handling aspects in R&D hotlabs. There is another technical issue concerning the oxidation pattern of carbides: the ability to reach the low oxygen level specification for manufactured products.

To understand the basic features and the main parameters governing the oxidation of (U, Pu)C, it is necessary to further examine the mechanisms involved, focussing on the behaviour of powdered or porous samples. The first part of this paper discusses a critical literature review, which establishes the state of the art in the field, while demonstrating the general lack of knowledge and highlighting uncertainties. Our experimental results are then discussed taking into consideration a basic theoretical kinetic treatment. To conclude this paper, practical solutions are proposed to safely deal with mixed (U, Pu) carbide fuel.

2. Literature review

2.1. Overview

Although the behaviour of UC_x fuel oxidation has been widely studied [1–5], data on the oxidation of (U, Pu)C fuel are scarce and not always useful or suitable. Only five references were found on the oxidation of (U, Pu)C fuel in oxygen containing gases [6–10]. Table 1 summarises the experimental conditions applied in these papers. The overall oxidation reaction is generally described as:

$$MC_x + O_2 \Rightarrow MO_x + C/CO_2 \tag{1}$$

in which M = (U, Pu), usually with 80 at.% U and 20 at.% Pu. The reactant carbide MC_x is assumed to be a two-phase mixture of monocarbide MC (90 wt.%) and sesquicarbide M_2C_3 (10 wt.%), without any free carbon. Regarding thermodynamic considerations, the equilibrium oxygen pressure over the carbides is obviously very low – not actually commensurable – and the oxidation is energetically very favourable ($\Delta_r H_{Ox} \sim -1250\ \mathrm{kJ/mol^{-1}}$ [7,9]). This induces a highly exothermic behaviour and defines one of the main technological challenges to overcome. Currently, U–Pu–C [11] and U–Pu–O are both complex ternary systems that remain to be fully determined. It is worth noting that the extent of oxygen solubility in MC – forming a poorly-known oxycarbide MC_xO_{1-x}, – is significant and increases with the Pu/U content in the MC phase (from ≈35 at.% in UC to ≈65 at.% in PuC) [11].

Two more articles of interest [12,13] deal with the XRD analysis of mixed carbide phases. Learning about the fine structure and composition of phases requires coupling chemical analysis (gas analysis on reduction melting, Kjeldhal method for nitrogen, mass spectroscopy) with structural characterisation (advanced XRD diffractometry) in order to provide an accurate assessment.

All the available literature was researched in order to collect relevant, reliable kinetic information on the oxidation of UC_x. The general idea was to provide relevant data for comparing the oxidation of UC_x and UPuC.

---

* Corresponding author. Tel.: +33 442 253 675; fax: +33 442 254 717.
E-mail address: fabrice.mazaudier@cea.fr (F. Mazaudier).

0022-3115/$ - see front matter © 2010 Elsevier B.V. All rights reserved.
doi:10.1016/j.jnucmat.2010.07.041

2.2. Oxidation behaviour

2.2.1. General trends

The oxidation products always consist of a voluminous and finely-divided oxide powder (specific surface area ≈ 1–5 m^2/g) made of two oxides, MO_{2+x} and M_3O_8, with the MO_2/M_3O_8 ratio depending on the oxidation temperature, the Pu content in the reactant, and the nature of the oxidising gas. The air oxidation process leads to a ratio ranging between 69/31 at 510 °C and 34/66 at 790 °C for each phase [6]. Assuming complete oxidation of carbon to CO_2, the weight gain of the oxidation lies between 8 and 12 wt.% according to the MO_2/M_3O_8 oxide ratio in the final product. This is an average range considering the fact that there is significant Pu enrichment in the MO_2 due to Pu depletion in the M_3O_8 (max. 5% Pu) at high temperature and that the behaviour of carbon is not well-known.

The higher the oxidation temperature in air, the lower the carbon content in the oxides [6]. The carbon content is 11,000 ppm in air at 350 °C (4 h), while it does not exceed 250 ppm at 790 °C (2 h) [6]. The residual carbon content in oxides is known to be higher after oxidation with CO_2 [7].

2.2.2. Kinetic aspects

Sintered carbide samples follow a linear oxidation under isothermal conditions in air, oxygen or carbon dioxide [1,7]. The oxidation rate depends on the oxygen content in a pseudo-affine relationship and increases only slightly with the temperature except in CO_2, where the temperature effect is more pronounced. The process is first accompanied by a linear weight gain and then by a weight loss whose amplitude rises with the temperature between 700 and 900 °C, a phenomenon called overshoot [1]. The low apparent activation energy of $\sim$20 kJ/mol derived from the figures reported by Matzke [1] for air oxidation is very low. This is especially true for the surface-controlled kinetics compared with the usual order of magnitude for this type of control, which is typically $\sim 10^2$ kJ/mol. Using low oxygen contents (10^{-4}–10^{-2} atm), Naito et al. [2] reported that the chemically-controlled oxidation kinetics of UC_x were located between 400 and 800 °C with a low apparent activation energy and U_3O_8 as a final oxidation product [2]. Above 800 °C, UO_{2+x} was the main oxidation product and the apparent activation energy dramatically increased from $\sim$7 to $\sim$100 kJ/mol [2]. In another paper, Mukerjee et al. [3] reported chemical or diffusion limiting steps to limit the oxidation process of UC (non-isothermal, 1–10 °C/min) under an atmosphere with a high oxygen content and with high apparent activation energy. It is worth noting that the temperature range investigated by these authors (200–500 °C) partially overlays those investigated by Naito et al. [2] but produces very different oxidation mechanisms. During the non-isothermal oxidation process starting from room temperature, the formation of an adherent and diffusion-limiting oxide film at low temperature determines the kinetics at higher temperature [3] regardless of the experimental kinetic barriers crossed, e.g. 400 °C. U_3O_8 is also described as the final product according to Naito et al. [2]. It is important to point out that for UC_x oxidation, the kinetics is determined by the oxide layer depending on its ability to mask/shield the reactive area [5] or, on the contrary, to form low-density and voluminous non-adherent powder.

The morphology of the oxide or oxycarbide layer determines the behaviour and drives the process to self-sustain if it is adherent and diffusion-limiting. The oxidation product of (U, Pu)C is known to be a voluminous and finely-divided oxide powder.

2.2.3. Oxidation hazards: pyrophoricity, breakaway kinetics and exothermicity

As examples of self-sustaining or divergent oxidation behaviours, two cases are well-known in the literature: the oxidation of metallic uranium [15] and the pyrophoricity of metallic plutonium [16,17]. Two aspects of the oxidation behaviour of metallic uranium and plutonium are similar, leading to the kinetic transition and possibly to pyrophoricity: high oxidation enthalpy and the parabolic growth of a compact oxide layer which reaches critical thickness and cracks (U) or spalls (Pu), including the significant self-heating of samples (Adda [15] reported an surtemperature (overheating above the temperature setpoint) of ≈200 °C for the oxidation of uranium ingots) and an average rate increasing over time in both cases. As a summary, the basic physico-chemical features of an M/O_2 reactive system with the ability to to self-sustain or diverge during oxidation are : (i) adherent, protective oxide layer, (ii) high apparent activation energy, (iii) unpredictable oxide layer breakaway (cracking or spallation) events, and (iv) high oxidation enthalpy. Such divergent behaviour has never been reported for the oxidation of (U, Pu)C.

2.2.4. Carbon oxidation

The study by Naito et al. [2] on UC oxidation highlights the significance and the role of the oxidation of carbon released and of the oxycarbide as an intermediate species. An overshoot similar to those reported by Matzke [1] for (U, Pu)C oxidation in CO_2 is described during the oxidation of sintered of UC_2 [4]. In the reaction route, Nawada et al. [4] shows that the carbon oxidation in UC_2 proceeded in two stages. Firstly, the lattice carbon released by oxidation is oxidised which is then followed by delayed oxidation on the excess residual carbon in as-manufactured samples. Among the oxide products, UO_3 is formed and then reduced to U_3O_8 by the carbon.

The oxidation behaviour of carbon in the (U, Pu)C lattice has never been described. It is known that graphite oxidation is widely influenced (catalysis effect) by the presence of uranium or plutonium oxides [14].

2.2.5. Glove-box handling and soft oxidation at room temperature

Lewis [9] provided an interesting DSC study on the oxidation behaviour of (U, Pu)C, simulating different kinds of oxygen incursions in a glove-box. The main result was that a powder bed can undergo an oxidation transient at room temperature with a sudden oxygen incursion without any self-sustaining process. His paper also clearly demonstrates that it is always necessary to heat samples to observe quantitative oxidation and eventually allow the reaction to go further. Similarly, Benedict et al. [6] shows the feature of an extinguishing reaction, which is only re-activated with the increasing temperature and oxygen content in the gas. Specific vibration boats were shown to be useful to accelerate oxidation even at high temperature [6,8]. Nevertheless, using batches of several hundreds of grams [6,7], one have to pay attention to the exothermicity of the reaction. The minimum temperature required to activate oxidation as assessed by Lewis [9] is over 150 °C for powdered samples and 300 °C for green solids. To answer the safety questions related to pyrophoricity, many authors recommend measuring this activation temperature in terms of ignition safety criteria, which is a mistake from a thermodynamic and kinetic viewpoint.

Oxidation also has to be managed, slowed down, or at least controlled when performing specific manufacturing steps like milling or machining at room temperature in glove-boxes. These operations create fresh reactive surfaces that act as efficient oxygen getters and unfortunately greatly increase the oxygen content of the final products. This ongoing oxidation is difficult to prevent. Cragg et al. [10] demonstrated the considerable influence at room temperature of small amounts of water vapour as glove-box atmosphere impurities, leading to a linear and continuous oxidation process of fresh carbide, while the oxidation process obeyed a parabolic-type rate law and reached an asymptotic weight gain value

(+1.2 wt.%) with oxygen present. Besides the conclusion on the room temperature oxidation degradation, Gragg et al. [10] do not report any pyrophoric behaviour of the powder even though their experimental set-up was among the worst in terms of the reactive area (10–20 cm^2 spread powder) exposed to the oxidant and gas renewal rate (5 s^{-1}).

2.2.6. Findings and discussion

The following main results were drawn from the literature review: (i) oxidation of (U, Pu)C always leads to the formation of finely-divided oxide that tends to slow down the process; (ii) solid samples obey linear kinetics in isothermal conditions, while the oxidation of powders is not described; (iii) the temperature does not dramatically influence the kinetics in air; (iv) neither self-sustaining nor igniting events were observed; (v) oxidation of UPuC does not reveal any kinetic transition; and (vi) development of vibrating devices, when used, are needed to accelerate, activate or achieve full oxidation. In standard hotlab facilities and inerted glove-boxes (≈10–100 ppm O_2 in N_2 or Ar), oxidation is thermodynamically possible but kinetically blocked at room temperature, except if a significant amount of water vapour is present.

The mechanisms behind the oxidation of (U, Pu)C were neither detailed nor discussed, even if comparison was sometimes made with the oxidation behaviour of UC_x. There is a lack of knowledge on the kinetics, the role of carbon, the oxidation behaviour of powdered samples and the possible explanation for the weak influence of temperature. Due to the complexity of the system, the reaction path of oxidation is undetermined *a priori* and not unique, as many phases are involved in the processus (see Fig. 1, to be compared with the U–Pu–C high temperature isothermal section reported by Matzke [1]). Authors generally do not consider the effect of annealing on the system when performing oxidation or the fact that the system is very far from equilibrium, i.e. metastable.

Among the information lacking in the literature, one can also regret the inadequate description of the experimental set-ups: the references reported above do not meet the quality criteria of analytic studies (see Table 1). While agreeing with Naito et al. [2], caution is needed before performing kinetic experiments and issuing any conclusive analysis.

3. Experimental procedure

3.1. Main objective

Specific analytic experiments were carried out to further explore the mechanisms of UPuC oxidation; firstly to check and to retrieve reported results, and secondly to obtain quantitative results on powdered and porous samples (reputed to be the most reactive) and to meet the main literature conclusions, e.g. the non-ability to self-sustain. Analytical isothermal (including pre and post-inerting) and non-isothermal ($dT/dt = 300–600$ °C/h) oxidation tests were performed on small samples (100–700 mg) in a Netzsch ThermoGravimetric Analyser STA429 at 500, 550, 600 and 700 °C with the oxygen content in the flowing gas ranging from 0.1 vol.% to 20 vol.%. Among experimental parameters listed in Tables 2 and 3, specific features of the oxidation behaviour have been taken into consideration and further discussed, e.g. the effect of N_2, the existence and the extent of local overtemperature, and the role of carbon.

3.2. Sample definition, oxidation set-up and parametric field

Various powdered and porous carbides were selected for the experimental programme (Table 2). Mixed uranium–plutonium carbide was obtained through the carbothermic reduction of a mixture of UO_2, PuO_2 and C at around 1500 °C in a vacuum or argon

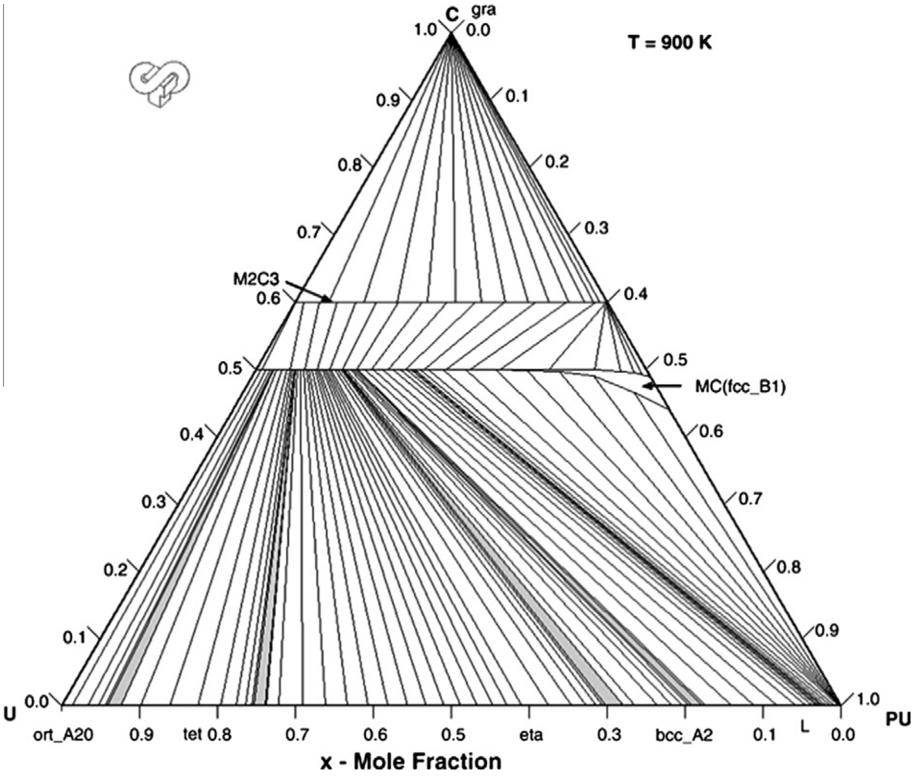

Fig. 1. U–Pu–C isothermal section at 627 °C [18].

Table 1
Experimental conditions used by previous investigators.

Refs.[a]	[5]	[6]	[7]	[8]	[9]
Sample	Sintered pellets (ϕ8, 5, h10)	Sintered pellets	Sintered "briquettes"	Powder (44–70 μm) green and sintered pellets	Powder(1–3 m^2/g)
TD[b] (other properties)	88–95% (3900 ppm O)	50, 85–96%	85–90%	50–97% (330–2300 ppm O)	–
Sample or batchweight	10–200 g	300–350 g	100–200 mg ?	13–70 mg	5 g
T (°C)	300–790	277–472	350–450	RT[c] to 600	RT[c]
Gas	Ar + 3–22% O_2	Ar + 25–60% O_2	Air, 100% O_2	Ar + 0.04–15.7% O_2	1–1000 ppm O_2 and/or H_2O
Oxidation set-up	Isothermal Non-isothermal (100 °C/h)	Isothermal	Isothermal	Non-isothermal (600 °C/h)	Isothermal
Equipment	Furnace	Furnace	?	DSC	Specific device Spread powder (10 or 20 cm^2)
Remarks	Batch experiments (big amount)	Batch experiments (big amount)	Lack of information on the experimental set-up	Specific transient experiments Gas cover, dT/dt	

[a] 15–20% Pu carbides except [6]: 70% Pu content samples.
[b] Theoretical density.
[c] Room temperature.

Table 2
Samples definition.

Samples (from carbothermic step)	Powder	Porous solid (clinker)
Density (g/cm^3)	3 (non-packed)	6.5
S_{BET} (m^2/g) (Micromeritics Flowsorb 2300)	1.7	1.8
Carbide phase content (%) and ratio (XRD, Siemens D5000)	~40–60 (bal.: mixed oxides, carbon)	>99
	$M_2C_3/MC \approx 90/10$	
Sample weight	20–700 mg (up to 2 g for a few batch experiments in "high quantity" tubular furnace)	
Remarks	Milled old (~1–5 yr) scraps Ar or N_2 calcination (600 °C) before each oxidation tests	Small millimetric fragment
50% porosity (25% opened)		

Table 3
Oxidation conditions.

Equipment	TGA thermobalance Netzsch STA 429	DSC calorimeter Netzsch DSC 404
Principle	Isothermal (pre- and post-inerting) Non-isothermal	
T (°C)	500; 550; 600; 700	500; 600
dT/dt (°C/h)	300 and 600	600
t (h)	1–10	
Sample weight (mg)	100–700	20–50
Gas	Ar + O_2 (0.01; 0.1; 1; 10; 20 vol.%)	Reconstitued air (80 vol.% N_2/20 vol.% O_2) Ar + O_2 (0.1; 1 vol.%)
Gas flow rate (ml/min)	50	40
Crucible	Al_2O_3 "trunk shape" V = 0.1 cm^3	Pt "plate shape" V = 0.05 cm^3

for 4 h, followed by sintering at around 1650 °C under a mixture of Ar + 8% H_2 for 10 h. All experiments were carried out in glove-boxes inerted with high-purity nitrogen (less than 50 ppm O_2).

The investigation was performed within a wide parametric field (Table 3).

Depending on what kind of information was required, thermogravimetric data were considered either in terms of weight change dm (mg), percentage $100 \times dm/m_o$ (%) (m_o the initial weight sample), or the extent of the reaction α expressed as $\alpha = dm/dm_{max}$ (dm_{max} the mass change at reaction completion).

3.3. Limitations

Further details on the structural or chemical quantitative analysis of the initial products are not given here due to: (i) the complexity of the quaternary system U–Pu–C–O, (ii) the variability of the powdered samples (old manufacturing scraps), and (iii) the high-level technical requirements for performing a quantitative analysis of samples (see [12,13]). Basic and commonly-accepted assumptions have already been given above. It is thought that the lack of knowledge on the systems and samples involved does not undermine the kinetic treatment described herein.

4. Results and discussion

4.1. General figures and trends

About forty experiments were performed and were shown to be reproducible. The average weight gain represented 5 ± 1 wt.% for the powdered samples and 11.8 ± 0.7 wt.% for the porous solids. Structural characterisation showed that, in both cases, the product was a powder composed of two oxide phases: $(U,Pu)O_2$ and $(U,Pu)_3O_8$. The MO_2/M_3O_8 ratio was situated between 60/40 at 500 °C, and 40/60 at 700 °C. The BET specific surface area of the oxide powder was 4.7 m^2/g, which is at least three times higher than the carbide sampled. Its non-packed density was ~1.6 g/cm^3. The oxidation heat was derived from isothermal DSC experiments performed on powdered samples at 500 °C and gave an estimation of 1500 kJ/mol. A particular observation was made for the porous solids where the formed oxide(s) did not adhere to the carbide and fell to the bottom of the crucible, forming small piles.

Isothermal TGA experiments for the powdered samples showed parabolic oxidation behaviour with a mass overshoot (see Fig. 2a). The solid samples obeyed pseudo-linear kinetics (see Fig. 2b) with a rate constant nearly proportional to the sample mass and to the oxygen content.

In both cases, the average oxidation rate did not increase considerably between 500 and 700 °C, confirming the weak influence of temperature. Low oxygen contents (from 100 ppm to 1 vol.% O_2) were also used and the oxidation tests performed led to the fol-

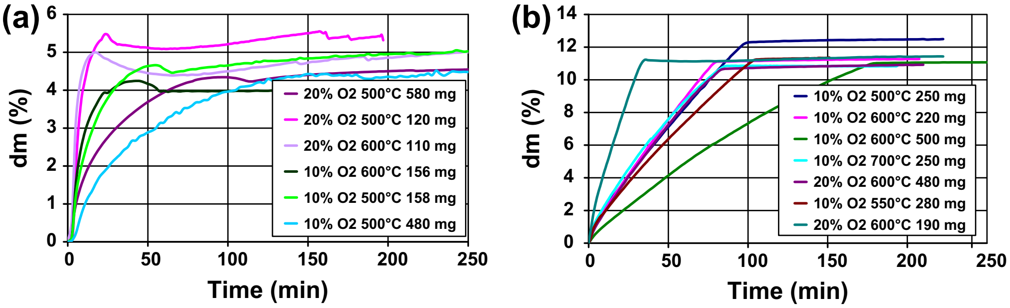

Fig. 2. Powdered (a) and porous (b) solid oxidation rate laws.

lowing conclusions: when detected, oxidation always obeys parabolic kinetics even for fresh carbide. Note that fresh carbide powder reacted readily with low oxygen contents (100 ppm) even at low temperature (60 °C) according to a parabolic rate law. The weight gain reached an upper limit of ~0.5 wt.% only, close to the value reported by Cragg et al. [10] (0.6–1.2 wt.%) without any auto-catalytic effect or kinetic transition.

N_2 calcinations of the powdered samples were performed to clean the samples and stabilize the mass before oxidation tests. They did not have any effect on the oxidation behaviour.

4.2. Overheating and self-sustaining ability

Thermal features of the reaction were carefully examined to answer the safety issues of exothermicity and pyrophoricity. Based on a precise analysis of each thermogram, the self-heating rate of the reacting powdered samples (TGA tests) was evaluated. The overtemperature was minor compared with the temperature setpoint, reaching only 4 or 8 °C in 10 and 20 vol.% O_2, respectively. The period of overheating for the powdered sample was nearly proportional to the mass involved. The surtemperature (overheating above the temperature setpoint) measured by Adda [15] during the oxidation of small metallic ingots of uranium was much higher, sometimes reaching 200 °C. However, considerable overheating (~100 °C) was detected during batch experiments with amounts of one to two grams of powdered carbide. This large difference is associated with the accessible surface area of carbide to the flowing oxygen ($\approx$300 mm^2 in the batch experiments vs. $\approx$10 mm^2 for the thermobalance crucible) and with the extent of the oxidation process in the beginning.

Different experiments were performed to check the ability of oxidation to self-sustain, e.g. DSC non-isothermal analysis (see Fig. 3) and isothermal TGA stop-heating tests which consisted in cutting off the heating of the device when oxidation reached steady-state conditions.

Depending on the accessible surface area of carbide, the activation temperature – assessed during non-isothermal testing (TGA and DSC) – was about 150 °C for the powdered samples and about 300 °C for the porous solids. Like many authors, we observed and confirmed that the oxidation of (U, Pu)C does not have the ability to self-sustain even at 500 °C in air. An example of oxidation extinction is shown in Fig. 3.

It proved that it is necessary to heat the sample each time in order to expedite oxidation.

4.3. Carbon behaviour

Regarding the oxidation of UC_2 reported by Nawada [4], the overshoot featuring the oxidation behaviour of powdered samples is caused by the oxidation of carbon in two steps. Firstly, the carbon released by the destruction of the carbide lattice, probably highly reactive, is oxidised practically at the same time as the metallic elements, U and Pu. Secondly, the excess carbon (graphitic form) is oxidised, as it was deduced from specific experiments discussed elsewhere [19] for an analytic indirect issue. As reported by Sampath et al. [14], actinide oxides greatly influence the oxidation kinetics of graphite, becoming quantitative above 500 or 600 °C, the range in which the phenomenon occurs.

5. Kinetic analysis

5.1. Powdered samples

5.1.1. Assumptions, models and limitations

Oxidation was assumed to proceed under quasi-isothermal-quasi-isobaric conditions considering that the *surtemperature* never exceeded 8 °C and the crucible was opened ($P \sim 1$ atm). For the kinetic analysis, the TGA oxidation of powdered samples (expressed in terms of the reacted fraction) was limited to an interval $\alpha \in [0.1\text{–}\approx 0.8]$ or smaller when required. In fact, only the ascendant part of the oxidation law was taken into account. The kinetic regime was supposed to be established and to proceed according to quasi-steady-state. The overshoot and the following part (weight loss) were not implemented in the kinetic treatment. It was also verified that the oxygen supply to the thermobalance always largely surpassed the possibility of consumption within the crucible. The reactant powder in the crucible was assumed to be a perfect cylinder made of a dense packing of spheres with a monomodal grain size distribution. Two important boundary conditions were defined to describe the reactive area: (i) the upper surface of the cylinder assumed to be a perfectly flat surface and (ii) the outer surface of each sphere. As the equilibrium oxygen pressure over the carbide was very low, it was assumed that nucleation was not rate-limiting. As the oxidation product cannot leave the crucible, we did not consider any surface- or interface-controlled modelling [20]. We used two basic analytical growth diffusion models [21], governing the relationship between the weight gain or the reacted fraction and time. The first model focussed on the crucible, while the second on the grain. The one-dimensional diffusion model $\alpha^2 = k_{(T)} \cdot t$ or $(\mathrm{d}m)^2 = k_{(T)} \cdot t$ (where t is the oxidation time) described the progression of the reaction front from the top to the bottom of the crucible with a constant reactive area. In this model, oxygen diffuses through the powder bed along a linear gradient. To assess the influence of the sample weight or the cylinder height, an extensity of the system, the weight gain data dm are more relevant than the reacted fraction α. At grain level, Jander's model and Ginstling–Brounshtein's model (GBM) were mainly used to model the diffusion-controlled reaction in a sphere [20]. These two grain-based models describe the shrinking of the carbide spherical core during transformation into a porous oxide. As Jander's model contains a number of weaknesses due to oversimplifications, we chose the GBM derived from Fick's second law, which is known to be more accurate. This model is represented by the following equation:

$$1 - 2/3\alpha - (1-\alpha)^{2/3} = k(T) \cdot t \quad (2)$$

5.1.2. Modelling application

The first model $dm^2 = k_{(T)} \cdot t$ does not correctly reproduce the oxidation behaviour of the bed powder in the crucible (see Fig. 4).

From this figure, it can be observed that the mass of powder – an extensive parameter of the system – has a considerable effect on the weight gain which increases with it. The reactive area cannot be described as a perfect disc moving down in the crucible. The reactive area obviously integrates part of the surface of each grain, deeper in the crucible early on in the oxidation process.

Let us consider the GBM (Eq. (2)) to implement the isothermal TGA data.

Regardless of the experimental conditions for the isothermal oxidation tests between 500 and 700 °C at 10 or 20 vol.% O_2 and with various sample masses, this model fits the experimental results as perfect straight lines, with an average correlation coefficient greater than 0.995 (see Fig. 5).

From these results, it was concluded that the kinetics were obviously grain-dependant. For a given temperature and oxygen content, the influence of the sample weight on the slope of the curves may be ascribed to the creation of an oxygen gradient between the top and bottom of the crucible.

The apparent activation energy was derived from a classical Arrhenius plot (see Fig. 6) based on GBM slopes for three tests (500, 600 and 700 °C) performed on equal amounts of powdered sample (~155–160 mg), the smallest but most reliable quantity used to minimize self-heating.

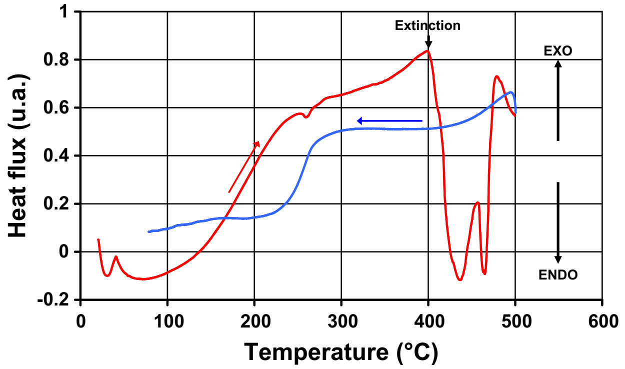

Fig. 3. Non isothermal cyclic (±10 °C/min) DSC curve (23 mg powdered sample, Ar + 1% O_2).

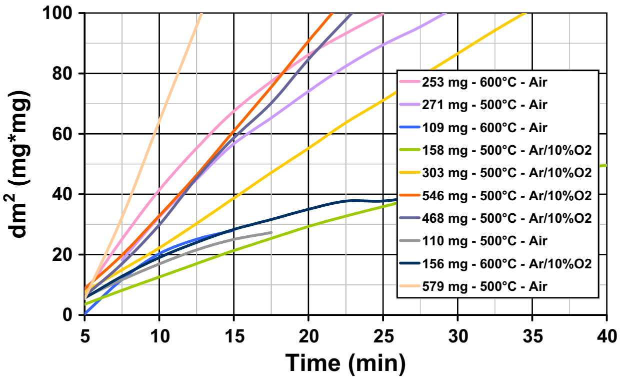

Fig. 4. Parabolic transforms $(dm)^2 = k_{(T)} \cdot t$.

The apparent activation energy measured was ~25 kJ/mol. This relatively low value – close to that estimated from the data reported by Matzke [1] – reflects the major role of gas transport. Fig. 7 illustrates the oxidation route of the powdered samples in the TGA crucible.

The oxidation follows a mixed kinetic regime including two parallel diffusion stages: (i) the first stage occurs in the powder bed from up to bottom and (ii) the second stage occurs in the oxide layer surrounding each grain considering that the oxide products cannot leave the reactive area.

Implementing this type of treatment to deal with kinetics is a preliminary valid approach which is sufficient to meet our requirements. However, the complete determination of any reaction path is far more complex, as many parameters and data have to be integrated [22,23], especially when powder is involved.

5.2. Porous solid samples

Modelling the oxidation behaviour of porous solid samples proved rather difficult, as the evolution of the fragment geometry was not known and impossible to predict. Nevertheless, pseudo-linear oxidation laws could be related to the chemical or interfacial control of the oxidation. This assumption was in good agreement with the observed fact that the formed oxide did not remain on the solid carbide surface, with no possible limitation on oxygen transport as in the case of powders.

Once again, the estimated apparent activation energy did not exceed 10 kJ/mol, which is an unusual and quite low value considering the chemically-controlled kinetics. This uncommon behaviour could be explained by the existence of a complex interfacial mechanism involving at least one or two exothermic and kinetically undistinguishable rapid steps (e.g. dissociative chemisorption of O_2, soft oxidation leading to the formation of an oxycarbide MCO), before a third limiting step leading to the formation of the final voluminous oxide products. The energy released by the stages preceding the limiting stage reduces the apparent activation energy, thus leading to the particularly low values measured.

6. Conclusion and practical solutions

The experimental results discussed in this paper are in very good agreement with the data available in the literature that we reviewed. The oxidation of mixed (U, Pu)C carbides (porous and powdered samples) in our experiments did not show any intrinsic ability to self-sustain regardless of the temperature or the oxygen content. Spontaneous and uncontrolled oxidation was never observed. On the contrary, heating was required to complete oxidation. The oxidation process does not show any unwanted kinetic transition. The oxidation products are always low-density finely-divided oxide powders expanding and tending to slow down oxidation: no protective oxide layer was observed on the samples.

In addition to the general figures and trends, new and original experimental results were collected for powdered samples, the role of carbon, and the effect of N_2. The kinetic treatment of isothermal TGA data proved that the apparent activation energy is low and confirmed the minor effect of temperature on the oxidation rate. Gas diffusion was assumed to play a major role in the oxidation process of powdered samples. As a general rule, managing oxidation has to be based on the oxygen availability.

6.1. Safety issue dealing with room temperature handling

At room temperature, handling in standard N_2-inerted gloveboxes (≈10–100 ppm O_2) does not represent any risk in terms of sudden and uncontrolled oxidation.

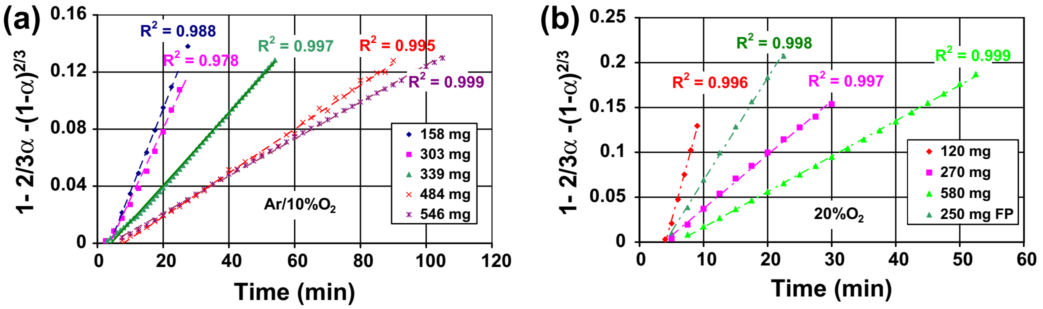

Fig. 5. GBM modelling of the experimental data obtained at 500 °C: (a) in Ar + 10 vol.% O_2 and (b) in N_2 + 20 vol.% O_2.

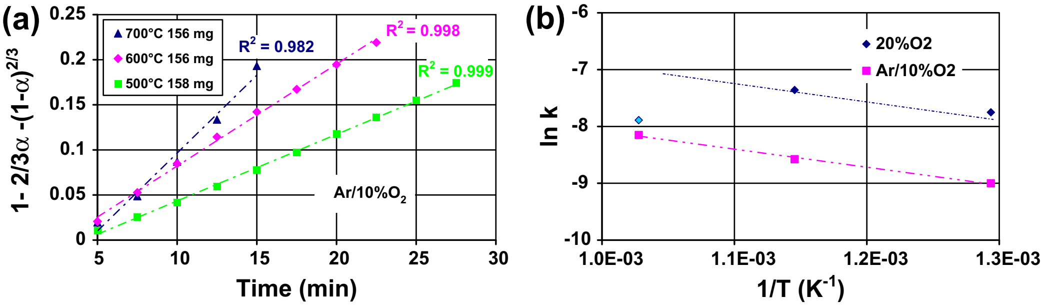

Fig. 6. Modelling of the experimental data at 500, 600 and 700 °C. (a) GBM modelling and (b) Arrhenius plots.

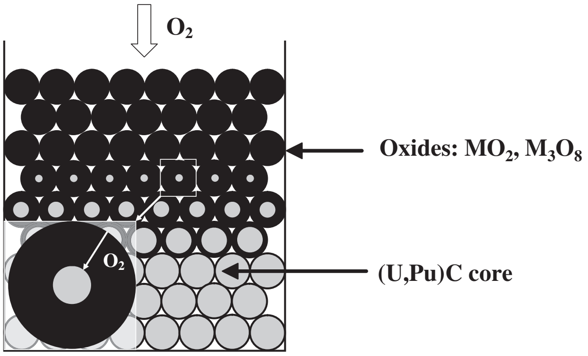

Fig. 7. Schematic representation of the powder oxidation route, from the top to the bottom within the crucible.

6.2. Oxygen content of manufactured carbides

Attention has to be paid to the water vapour content in the glove-box in order to limit the oxygen content in the carbothermic solid (clinker) during milling before the sintering step and to reach the quality target. It also seems preferable to inert the glove-box atmosphere with Ar seems rather than N_2 in order to prevent any oxy-carbo-nitrides from forming, even if there is no reliable evidence of any damaging or catalytic effect of nitrogen on oxidation.

6.3. High-temperature oxidation process

The oxidation process determined for the oxide conversion of mixed (U, Pu)C consists of isothermal oxidation above $T = 600$ °C in a high oxygen content atmosphere, carried out with pre- and post-inerting steps. The choice of a relatively high-temperature oxidation treatment is a compromise between performance, efficiency, safety, and the specification of the oxide products. This compromise is necessary to reduce the carbon content as much as reasonably achievable and to obtain a real recyclable powder. CO_2 evolution at high temperature help dissipate the energy and prevent an adherent layer from forming.

In the future, oxide conversion will be performed in a multi-purpose tubular alumina furnace. Monitoring will be based on the continuous analysis of O_2 and CO_2 upstream and downstream of the reactor, and on a controlled oxygen supply. To manage exothermicity and any abnormal events, sensors (temperatures, pressure, cooling system flow) and feedback actuators will be used to track the oxygen availability. A specific device is also currently being developed to improve the safety process.

References

[1] Hj Matzke, Science of Advanced LMFBR Fuels, North Holland Physics Publishing, Elsevier Science Publishers, B.V., 1986.
[2] K. Naito, N. Kamegashira, et al., J. Nucl. Sci. Technol. 13 (5) (1976) 260–267.
[3] S.K. Mukerjee, G.A. Rama Rao, J.V. Dehadraya, V.N. Vaidya, V. Venugopal, J. Nucl. Mater. 210 (1994) 97–106.
[4] H.P. Nawada, P. Srirama Murti, G. Seenivasan, S. Anthonysamy, C.K. Mathews, J. Therm. Anal. 35 (1989) 1145–1155.
[5] F. Le Guyadec, C. Rado, S. Joffre, S. Coullomb, C. Chatillon, E. Blanquet, J. Nucl. Mater. 393 (2009) 333–342.
[6] U. Benedict et al., Trans. Am. Nucl. Soc. 31 (1979) 512.
[7] V.S. Iyer et al., Nucl. Technol. 91 (1990) 389–393.
[8] P. Novoselov et al., Atom. Energiya 53 (2) (1982) 77–80.
[9] H.D. Lewis, in: Proc. of Intl. Meet. on Adv. LMFBR Fuels, Tucson, Arizona, USA, October, 1977.
[10] D.G. Cragg, R.J. Dicker, J.D.L. Harrison, J.W. Isaacs, J.R. Laren, W.T.G. Roberts, Bull. Soc. Française Céram. 77 (11–12) (1967).
[11] P.E. Potter, J. Nucl. Mater. 42 (1972) 1–22.
[12] R. Lorenzelli, P. Delaroche, J. Appl. Cryst. 5 (1972) 267–270.
[13] G.C. Jain, C. Ganguly, J. Nucl. Mater. 207 (1993) 169–176.
[14] S. Sampath, N.K. Kulkarni, M.S. Subramanian, N.C. Jayadevan, Carbon 26 (2) (1988) 129–137.
[15] Y. Adda, Rapport CEA-R-757, 1958.
[16] Joseph C. Martz, John M. Haschke, J. Nucl. Mater. 210 (1994) 130–142.
[17] T.C. Totemeier, USA/DOE/ANL/ED/95-2 Report, 1995.

[18] E. Fisher, Calphad 33 (2009) 487–494.
[19] Alan Handschuh, in: STPMF 2009 Conference, Montpellier, France.
[20] A. Fèvre, M. Murat, J. Therm. Anal. 7 (1975) 446.
[21] A. Fèvre, M. Murat, J. Therm. Anal. 7 (1975) 430.
[22] P.K. Gbor, Charles Q. Jia, Chem. Eng. Sci. 59 (2004) 1979–1987.
[23] S. Perrin, PhD thesis, Ecole des Mines de Saint-Etienne, 2002.